RECLAMATION

Managing Water in the West

Improved modeling of complex sediment processes using experimental data and laboratory measurements

Research and Development Office
Science and Technology Program
(Final Report) ST-2019-1778-01

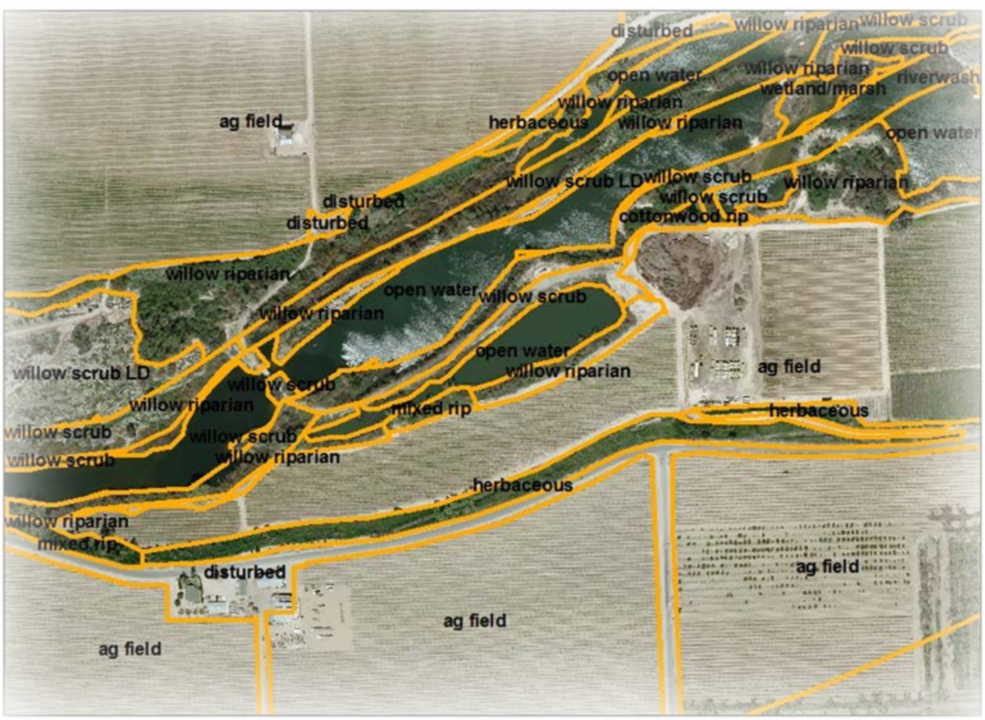

U.S. Department of the Interior
Bureau of Reclamation
Research and Development Office

October 2019

Mission Statements

The Department of the Interior conserves and manages the Nation's natural resources and cultural heritage for the benefit and enjoyment of the American people, provides scientific and other information about natural resources and natural hazards to address societal challenges and create opportunities for the American people, and honors the Nation's trust responsibilities or special commitments to American Indians, Alaska Natives, and affiliated island communities to help them prosper.

Disclaimer:

This document has been reviewed under the Research and Development Office Discretionary peer review process https://www.usbr.gov/research/peer_review.pdf consistent with Reclamation's Peer Review Policy CMP P14. It does not represent and should not be construed to represent Reclamation's determination, concurrence, or policy.

REPORT DOCUMENTATION PAGE		*Form Approved* *OMB No. 0704-0188*
T1. REPORT DATE: OCTOBER 2019	**T2. REPORT TYPE:** RESEARCH	**T3. DATES COVERED**
T4. TITLE AND SUBTITLE Improved modeling of complex sediment processes using experimental data and laboratory measurements		**5a. CONTRACT NUMBER** XXXR4524KS-RR4888FARD170020003 **5b. GRANT NUMBER** **5c. PROGRAM ELEMENT NUMBER** 1541 (S&T)
6. AUTHOR(S) Daniel Dombroski, ddombroski@usbr.gov		**5d. PROJECT NUMBER** ST-2019-1778-01 **5e. TASK NUMBER** **5f. WORK UNIT NUMBER** 86-68240
7. PERFORMING ORGANIZATION NAME(S) AND ADDRESS(ES) Bureau of Reclamation, Denver Technical Service Center, 6th Ave & Kipling St., PO Box 25007, Denver, CO 80225		**8. PERFORMING ORGANIZATION REPORT NUMBER**
9. SPONSORING / MONITORING AGENCY NAME(S) AND ADDRESS(ES) Research and Development Office U.S. Department of the Interior, Bureau of Reclamation, PO Box 25007, Denver CO 80225-0007		**10. SPONSOR/MONITOR'S ACRONYM(S)** **R&D:** Research and Development Office **BOR/USBR:** Bureau of Reclamation DOI: Department of the Interior **11. SPONSOR/MONITOR'S REPORT NUMBER(S)** ST-2019-1778-01

12. DISTRIBUTION / AVAILABILITY STATEMENT
Final report can be downloaded from Reclamation's website: https://www.usbr.gov/research/

13. SUPPLEMENTARY NOTES

14. ABSTRACT *(Maximum 200 words)*
Sedimentation is inclusive of the processes by which clay, silt, sand, and gravel are eroded, transported, and deposited. Understanding the sedimentation process and how to manage it requires the ability to accurately predict, control, and monitor sediment transport. The development of numerical modeling tools to quantitatively simulate sediment processes is key to Reclamation's ability to understand historical events and predict the effect of future management changes on sedimentation. The challenge is underscored by the increasing priority of maintaining ecosystem function while sustaining water supply and providing flood production. The research herein builds upon prior work at Reclamation's TSC by incorporating detailed measurements from laboratory flume experiments to improve the ability to numerically model complex sedimentation processes such as those created through the interaction with riparian vegetation. We propose that the formulations for estimating sediment transport capacity be modified to incorporate the effects of stem-generated turbulence, which have shown to be a dominant mechanism for mobilizing sediment in vegetated flow conditions. The final model will allow for more realistic simulation of sediment transport, erosion, and deposition for use in river restoration design.

15. SUBJECT TERMS Vegetated flow, sediment transport model, sediment modeling, echohydraulics

16. SECURITY CLASSIFICATION OF:	**17. LIMITATION OF ABSTRACT** U	**18. NUMBER OF PAGES**	**19a. NAME OF RESPONSIBLE PERSON** Daniel Dombroski

a. REPORT	b. ABSTRACT	c. THIS PAGE			19b. TELEPHONE NUMBER
U	U	U			303-445-2570

S Standard Form 298 (Rev. 8/98)
P Prescribed by ANSI Std. 239-18

BUREAU OF RECLAMATION

Research and Development Office
Science and Technology Program

Sedimentation and River Hydraulics Group, Denver Technical Service Center, 86-68240

(Final Report) ST- 2019-1778-01

Improved modeling of complex sediment processes using experimental data and laboratory measurements

DANIEL DOMBROSKI Digitally signed by DANIEL DOMBROSKI Date: 2019.10.04 13:26:34 -06'00'

Prepared by: Daniel Dombroski, Ph.D., P.E.
Hydraulic Engineer, Sedimentation River Hydraulics Group

MICHAEL SIXTA Digitally signed by MICHAEL SIXTA Date: 2019.10.04 13:31:19 -06'00'

Peer Review: Michael Sixta, M.S., P.E.
Hydraulic Engineer, Sedimentation and River Hydraulics Group,

For Reclamation disseminated reports, a disclaimer is required for final reports and other research products, this language can be found in the peer review policy:
This document has been reviewed under the Research and Development Office Discretionary peer review process https://www.usbr.gov/research/peer_review.pdf consistent with Reclamation's Peer Review Policy CMP P14. It does not represent and should not be construed to represent Reclamation's determination, concurrence, or policy.

Executive Summary

Predicting the effects of riparian vegetation on hydraulics and sediment transport within managed riverine systems is a growing challenge due to the increasing priority of maintaining ecosystem function while sustaining water conveyance. Quantitative predictive tools are needed to aid the science, economics, and policy of establishing environmental flows by addressing questions regarding the physical interaction of flow, vegetation, and sediment in rivers and floodplains.

A quantitative two-dimensional model (Dombroski D. E., 2017; Dombroski D. E., 2014) has been developed at the Technical Service Center for simulating the effect of vegetation characteristics on river and floodplain hydraulics through spatially distributed roughness. The model is based upon the SRH-2D package (Lai, 2010), which contains a two-dimensional flow and mobile bed sediment transport model. The vegetation-hydraulic solver uses measured vegetation parameters and calculated hydraulic variables to estimate a spatially-distributed, dynamic roughness coefficient that is coupled to the simulated hydrodynamics through the bed shear stress. Quantifying transport of sediment under vegetated flow conditions presents additional challenges because the mechanical processes driving sediment mobility may differ greatly than that under uniform flow conditions for which predictive formulas are traditionally developed. For example, increasing roughness to account for hydraulic resistance may cause gross inaccuracies in predictions of sediment transport capacity because the assumed linkage between roughness at the bed and fluid force is no longer valid. Although the total sediment load equations perform well in simulating transport under uniform flow conditions, the lack of direct linkage to some important flow characteristics (e.g., turbulence production due to interaction with objects and complex geometries) limits the practical applicability to conditions under which the effects are small. To be able to address the increasingly common sedimentation issues associated with more complex flow geometries and vegetated conditions, further development of the theoretical framework upon which the sediment transport models are based is necessary. Sediment transport under complex flow conditions has been studied in the laboratory setting to develop a better understanding of the interactions and important parameters governing transport rates and distributions. We incorporate measurements of hydraulic variables and sediment flux from a flume study to inform conditions under which the computational model lacks proficiency. A formulation for driving sediment mobility is proposed that incorporates the effects of stem-generated turbulence in order to better capture the dominant mechanisms under vegetated flow conditions. The developments will increase the usability and accuracy in simulating vegetation effects on hydraulics and sediment transport. Further testing, validation, and refinement of the model will continue as it is applied at the project level.

Contents

Figures

Introduction

Sedimentation is inclusive of the processes by which clay, silt, sand, and gravel are eroded, transported, and deposited. Sedimentation is one of the most significant problems facing the management of rivers and reservoirs today; it is responsible for loss of conveyance, reduced flood protection, reduced power generation capacity, and ecosystem degradation. Fundamentally, the issue of reservoir sustainability is a matter of managing sedimentation. Understanding the sedimentation process and how to manage it requires the ability to accurately predict, control, and monitor sediment transport. Understanding transport of sediment is also critical to the design of river restoration strategies that involve the engineered manipulation of channel geometry and riparian vegetation. Quantitative understanding of linkages between vegetation and sediment transport is necessary in order to design sustainable river restoration projects.

Predicting the effects of riparian vegetation on hydraulics and sediment transport within managed riverine systems is a growing challenge due to the increasing priority of maintaining ecosystem function while sustaining water conveyance. Quantitative predictive tools are needed to aid the science, economics, and policy of establishing environmental flows by addressing questions regarding the physical interaction of flow, vegetation, and sediment in rivers and floodplains. These tools are especially critical for regions of the Western U.S. like Central California, in which multi-benefit water projects (e.g., projects that enhance flood safety, wildlife habitat, and public recreation) are legally mandated components of regional and State-wide planning and funding efforts. These multi-benefit projects can be critically dependent on accurate estimates and modeling of vegetation effects on hydraulic conveyance, due to concerns over increases in roughness resulting from vegetation establishment and growth.

Numerical modeling tools (e.g., SRH-1D, SRH-2D, U2RANS) developed at Reclamation (Lai Y. G., 2010; Huang & Greimann, 2012) are commonly used to simulate flow and sediment transport in order to predict effects of management changes on sedimentation in rivers and reservoirs. These quantitative predictive tools have been valuable in understanding and comparing outcomes of management alternatives; however, the complexity of issues that Reclamation faces is growing with an increasing priority of maintaining ecosystem function while sustaining water supply and providing flood protection. Growing challenges call for continued development of tools that can better predict the effects of complex ecohydraulic processes related to sediment transport in the riparian environment. Current sediment modeling tools do not directly account for the effect of riparian vegetation on sediment processes and therefore it is difficult to quantify the effect of riparian restoration design on channel processes or to estimate the sustainability of a specific design.

Theoretical Background

SRH-2D Model Overview

A quantitative two-dimensional model (Dombroski D. E., 2014) is in active development at Reclamation's Technical Service Center for simulating the effect of riparian vegetation on hydraulics and sediment transport in the river and floodplain environment. The model is based upon the SRH-2D package (Lai, 2010), which contains a two-dimensional flow and mobile bed sediment transport model. Hydraulic variables are computed by solving the depth-averaged dynamic wave (St. Venant) equations using a finite volume numerical method:

$$\frac{\partial h}{\partial t}+\frac{\partial hU}{\partial x}+\frac{\partial hV}{\partial y}=e \tag{1}$$

$$\frac{\partial hU}{\partial t}+\frac{\partial hUU}{\partial x}+\frac{\partial hVU}{\partial y}=\frac{\partial hT_{xx}}{\partial x}+\frac{\partial hT_{xy}}{\partial y}-gh\frac{\partial z}{\partial x}-\frac{\tau_{bx}}{\rho}+D_{xx}+D_{xy} \tag{2}$$

$$\frac{\partial hV}{\partial t}+\frac{\partial hUV}{\partial x}+\frac{\partial hVV}{\partial y}=\frac{\partial hT_{xy}}{\partial x}+\frac{\partial hT_{yy}}{\partial y}-gh\frac{\partial z}{\partial y}-\frac{\tau_{by}}{\rho}+D_{yx}+D_{yy} \tag{3}$$

In the above, t is time, x and y are horizontal Cartesian coordinates, h is water depth, U and V are depth-averaged velocity components in x and y directions, respectively, e is excess rainfall rate, g is gravitational acceleration, T_{xx}, T_{xy}, T_{yy} are depth-averaged turbulent stresses, D_{xx}, D_{xy}, D_{yx}, D_{yy} are dispersion terms due to depth averaging, $z = z_b + h$ is water surface elevation, z_b is bed elevation, ρ is water density, and τ_{bx}, τ_{by} are the bed shear stresses (friction). Bed shear stresses are calculated by the SRH-2D hydraulic solver that uses the Manning's roughness equation as follows:

$$\begin{pmatrix}\tau_{bx}\\ \tau_{by}\end{pmatrix}=\rho C_f\begin{pmatrix}U_x\\ U_y\end{pmatrix}\sqrt{U_x^2+U_y^2}; \quad C_f=\frac{gn^2}{h^{1/3}} \tag{4}$$

where n is the Manning's roughness coefficient. The user-specified Manning's n is generally spatially-distributed yet independent of the computed hydraulic variables and is the primary "tuning" parameter used during model calibration. The turbulent stresses are computed through an enhanced viscosity (Boussinesq assumption):

$$T_{xx}=2(\nu+\nu_t)\frac{\partial U}{\partial x}-\frac{2}{3}k \tag{5}$$

$$T_{xy}=(\nu+\nu_t)\left(\frac{\partial U}{\partial y}+\frac{\partial V}{\partial x}\right) \tag{6}$$

$$T_{yy}=2(\nu+\nu_t)\frac{\partial V}{\partial y}-\frac{2}{3}k \tag{7}$$

where ν is kinematic viscosity of water, ν_t is the turbulent eddy viscosity, and k is the turbulent kinetic energy. One of two turbulence closure schemes is used to model the eddy viscosity: $\nu_t = C_t U_* h$ (parabolic model) or $\nu_t = C_\mu k^2/\varepsilon$ (k-ε model), where C_t and C_μ are constants, U_* is the bed frictional velocity, and ε is turbulent energy dissipation. Solution requires solving additional conservation equations for k and ε.

Sediment transport computations are performed within SRH-2D by solving a total load (combined bed and suspended load) conservation equation that attributes sediment concentration rate of change to the sum of the divergence of the sediment flux and the inequality between equilibrium and local transport rates (Greimann, Lai, & Huang, 2008):

$$\frac{\partial hC_k}{\partial t}+\frac{\partial \cos \propto_k \beta_k V_t hC_k}{\partial x}+\frac{\partial \sin \propto_k \beta_k V_t hC_k}{\partial y} = \frac{\partial}{\partial x}\left(hf_k D_{sx}\frac{\partial C_k}{\partial x}\right)+\frac{\partial}{\partial y}\left(hf_k D_{sy}\frac{\partial C_k}{\partial y}\right)+S_{e,k} \quad (8)$$

Equation (8) is valid for each sediment size class k, where C_k is depth-averaged sediment concentration, α_k is the direction angle of sediment transport, V_t is depth-averaged resultant flow velocity, D_{sx}, D_{sy} are sediment dispersion coefficients, f_k is the transport mode parameter ($0 \le f_k \le 1$), β_k is the sediment-to-flow velocity ratio, and $S_{e,k}$ is a source term accounting for sediment erosion and deposition:

$$S_{e,k}=\frac{1}{L_{t,k}}\left(q^*_{t,k}-\beta_k V_t hC_k\right) \quad (9)$$

In the above, $L_{t,k}$ is the adaptation length scale and $q^*_{t,k}$ is the equilibrium capacity sediment transport rate for size class k. The form of Equation (9) represents total load; pure bedload or suspended load formulas can be recovered by adjusting f_k and $S_{e,k}$ (Lai & Gaeuman, 2013) (Greimann, Lai, & Huang, 2008):

$$S_{e,k}=\zeta_k \omega_{s,k}\left(C^*_{s,k}-C_{s,k}\right), f_k=1 \text{ for suspended load}$$

$$S_{e,k}=\frac{1}{L_{b,k}}\left(q^*_{b,k}-q_{b,k}\right), f_k=0 \text{ for bedload}$$

A sediment transport capacity equation is needed to calculate $q^*_{t,k}$ in Equation (9); SRH-2D offers the user options to select from equations by Engelund-Hanson (1972), Meter-Peter and Muller (Modified; 1948), Parker (1990), Wilcock and Crowe (2003), Wu et al. (2000), and Yang (1973, 1979, 1984).

Vegetation, Hydraulics, and Sediment Transport

The SRH-2D package features the addition of a hydraulic roughness module for computing dynamic, spatially-distributed Manning's *n* values based on vegetation characteristics (Dombroski D. E., 2014). The computed Manning's *n* roughness values account for resistance due to form drag of flow through the vegetation. The vegetation module receives spatially-distributed input data via a user-generated ArcGIS shapefile that is automatically mapped to the computational grid of the hydraulic solver at runtime. The computational time step for the hydraulic solver is generally limited by numerical instability, whereas the computational time step for the vegetation module is limited by ecologically-relevant scales and can generally be significantly larger. A larger vegetation time step offers the benefit of decreased computational overhead.

The vegetated flow formulas of Baptist et al. (2007), Järvelä (2004), Kouwen & Li (1980), and Kouwen & Fathi-Moghadam (2000) are implemented in the model for calculating roughness. Each algorithm was developed based on theory and empiricisms to model a subset of vegetation types and flow conditions; the algorithms algebraically relate roughness to hydraulic variables and vegetation characteristics. Hydraulic variables are computed by the SRH-2D solver; however, vegetation characteristics must be measured and input to the model via an attribute table associated with the ArcGIS shapefile.

An inherent challenge associated with the vegetation modeling approach is that direct measurement of vegetation characteristics becomes unfeasible for large riparian corridors. On-the-ground field measurements are labor intensive (Gillihan, 2013) and are typically performed over subplots or across transects, leading to the necessity for statistical extrapolation to larger spatial extents. In order to meet the need for vegetation characteristics over the full modeled domain, the methodology of Mason et al. (2003) was adopted to estimate roughness based on remotely-sensed data. The approach (Dombroski D. E., 2017) demonstrated the practicality of informing the hydraulic model with vegetation characteristics deduced from LiDAR data, which is increasingly being collected as part of routine project scope and usually provides complete spatial coverage throughout the model domain.

The presence of vegetation within open channel flows generally increases inundation which can be accounted for in numerical modeling exercises by increasing the substrate roughness values as a function of the plant patch characteristics. The SRH-2D module simulates the effect of vegetation in this manner, dynamically adjusting Manning's *n* according to equivalent roughness formulations (Dombroski D. E., 2014). However, variation of the roughness to account for hydraulic resistance may lead to gross inaccuracies in predictions of the fluid capacity to mobilize sediment. Dombroski (2017) introduces a partitioned roughness approach that separates grain roughness used to compute sediment transport capacity from the total hydraulic roughness. The approach shows proficiency in modeling conditions under which flow through vegetation causes a trapping effect on sediment mobility. Although the bulk drag resistance of flow through vegetation has been shown to reduce bed shear stress (Lopez & Garcia, 1997; Thompson, Wilson, & Hansen, 2004), turbulence enhancement around stems can increase sediment entrainment locally for some spacing and geometry configurations (Nepf H. M., 1999; Nezu & Onitsuka, 2001), complicating the analysis.

The presence of vegetation effects the vertical distribution of velocities and near-bed stresses, which cannot generally be simulated through modification of the roughness alone. Flow within the vegetation zone is generally slow moving relative to that outside of the vegetation, which alters the near-bed shear stresses. For submerged vegetation, faster moving flow is partitioned above with high shear and turbulence levels at the interface (Simon, Bennett, & Neary, 2004; Le Bouteiller & Venditti, 2015). Turbulence intensity within the vegetation zone is highly dependent on the stem density and diameter and is generally an important mechanism driving sediment transport and dispersion (Tanino & Nepf, 2008). Without explicit consideration of the stresses induced by the presence of vegetation in the flow, such models are not entirely useful in predicting sediment transport effects (Larsen, 2008). An explicit treatment of the effect of vegetation characteristics on the intensity of turbulent fluctuations is needed in order to predict mass transport trends that are directly coupled.

Methods

Laboratory Flume Experiments

The influence of varying vegetation stem configuration on bedload transport rate was explored in a recirculating laboratory flume at Massachusetts Institute of Technology (Yang, 2018). Transport rate was measured in a bare channel and for vegetated conditions in order to infer dependencies on shear stress, turbulent kinetic energy, and vegetation solid volume fraction. Transport rate generally increased with vegetation solid volume fraction, even as shear stress was held constant, suggesting that stem-generated turbulence is an important mechanism for mobilizing sediment. Transport rate and turbulent kinetic energy generally scaled consistently across bare and vegetated conditions, suggesting potential for a more robust predictive relationship than conventional models dependent on shear stress. Details of the experimental setup, measurements, and results are presented in 1.

SRH-2D Hydraulic and Mobile Bed Model

An SRH-2D hydraulic and mobile bed sediment model was built to simulate the experiments conducted in the laboratory flume. The model is based on a 1 m wide by 10 m long rectangular grid comprised of 2000 quadrilateral cells. A single sediment gradation was specified having minimum, maximum, and median grain diameter of 0.42, 0.6, and 0.5 mm, respectively.

The model was calibrated to the bare bed (non-vegetated) flume experiments. For the non-vegetated simulations, a constant roughness was specified over the entire model domain. The model was considered calibrated when the mean velocity, depth of flow, and sediment transport rate approximately matched that reported in the results of the flume experiments.

The effect of vegetation on the hydraulics and sediment transport was modeled using several approaches. The Wilcock & Crowe (2003) formulation was selected for calculating transport capacity based on the calibration results. In comparison with the laboratory experiments, the results demonstrate that the model vastly underpredicts the sediment transport rate, regardless of the chosen formula, for estimating vegetative roughness. In the model, the total roughness is used to calculate the hydraulic variables while only the grain roughness component is used to compute sediment transport capacity (Dombroski D. E., 2017). The approach approximates the effect of sediment trapping, which effectively reduces the fluid capacity to move sediment, without consideration of potential for capacity enhancement due to vegetation-generated turbulence. Details of the model setup, simulations, and results are presented in 4.

Turbulence-Based Sediment Capacity

The results of the numerical modeling as compared to the experimental measurements motivate the need for a formulation of the fluid capacity needed to mobilize sediment that is based on strength of turbulent fluctuations. The mobility of sediment in open channel flow over an unvegetated bed is commonly taken to be dependent on the bed shear stress, which is in turn linearly related the turbulent kinetic energy (Yang, 2018). However, under vegetated flow conditions, the turbulence production is related to the vegetation characteristics; using shear stress as a determination of sediment mobility under such conditions may lead to spurious results.

Following the work of Yang (2018), we propose the adoption of a modified transport model based on an estimation of the turbulent kinetic energy in vegetated conditions. The formulation presented by Yang (2018) is a reinterpretation of the bedload transport Einstein-Brown model (Einstein, 1950; Brown, 1950),

$$Q_{s*} = \begin{cases} 2.15e^{-2.06/k_{t*}}, & k_{t*} < 0.95 \\ 0.27k_{t*}^3, & 0.95 < k_{t*} < 2.74, \end{cases} \quad (10)$$

where Q_s is the dimensionless bedload transport rate and k_{t*} is the dimensionless turbulent kinetic energy:

$$k_{\mathrm{t}*} = \frac{k_t}{(\rho_s/\rho - 1)gd_s} \quad (11)$$

Yang et al. (2016) proposed the following relationship for the near-bed turbulent kinetic energy k_t:

$$k_{\mathrm{t}} = \frac{C_f}{0.19}U^2 + 0.9C_D^{2/3}\emptyset^{2/3}U^2 \quad (12)$$

In the above, ρ_s is the grain density, d_s is grain diameter, U is mean channel velocity, $\emptyset$ is vegetation solid volume fraction, and C_D is the vegetation drag coefficient. The bed drag coefficient C_f is approximated from the water depth h and sediment size d_s as

$$C_f = \frac{1}{[5.75\log(2h/d_s)]^2} \quad (13)$$

The dimensional bedload transport rate Q_s can be recovered from the definition of the nondimensionalized quantity (Einstein, 1950):

$$Q_s = Q_{s*}\rho_s\omega_o d_s \tag{14}$$

The particle fall velocity ω_o is approximated as (Rubey, 1933):

$$\omega_o = \sqrt{gd_s(\rho_s/\rho - 1)}\left[\sqrt{\frac{2}{3} + \frac{36v^2}{(\rho_s/\rho - 1)gd_s^3}} - \sqrt{\frac{36v^2}{(\rho_s/\rho - 1)gd_s^3}}\right] \tag{15}$$

Using Equations (10)-(15), we estimate a new bedload transport rate using the hydraulic simulation results from the SRH-2D model (Appendix 4) and the sediment and vegetation characteristics as reported from the Yang (2018) laboratory experiments (Appendix 1). Shown in Figure 1 is bedload sediment transport rate Q_s as a function of the average channel velocity *U* for vegetation solid volume fractions ∅ = 0 (panel A), ∅ = 0.005 (panel B), and ∅ = 0.025 (panel C). Presented in each panel are results from the Yang (2018) laboratory experiments (black), the SRH-2D simulation results (orange), and the computed sediment transport rates as proposed in Equations (10)-(15) (gray). For the bare channel (non-vegetated) condition (∅ = 0), panel A shows that reasonable agreement is made in transport rates between both predictive models and the laboratory experiments. However, for the vegetated conditions (∅ = 0.005 and ∅ = 0.025), panels B and C show that the SRH-2D model vastly underpredicts the transport rate compared to the laboratory experiments. It is hypothesized that the underprediction is due to stem-generated turbulence, which mobilizes sediment in the laboratory environment, but is not accounted for in the SRH-2D model. Using Equations (10)-(15) to compute the sediment transport rate produced more reasonable agreement between predicted Q_s and laboratory measured Q_s, as shown in panels B and C. The predictions computed from the framework presented in Equations (10)-(15) used the depth of flow *h* and velocity *U* taken from the SRH-2D simulation results along with the known sediment characteristics and vegetation solid volume fraction ∅.

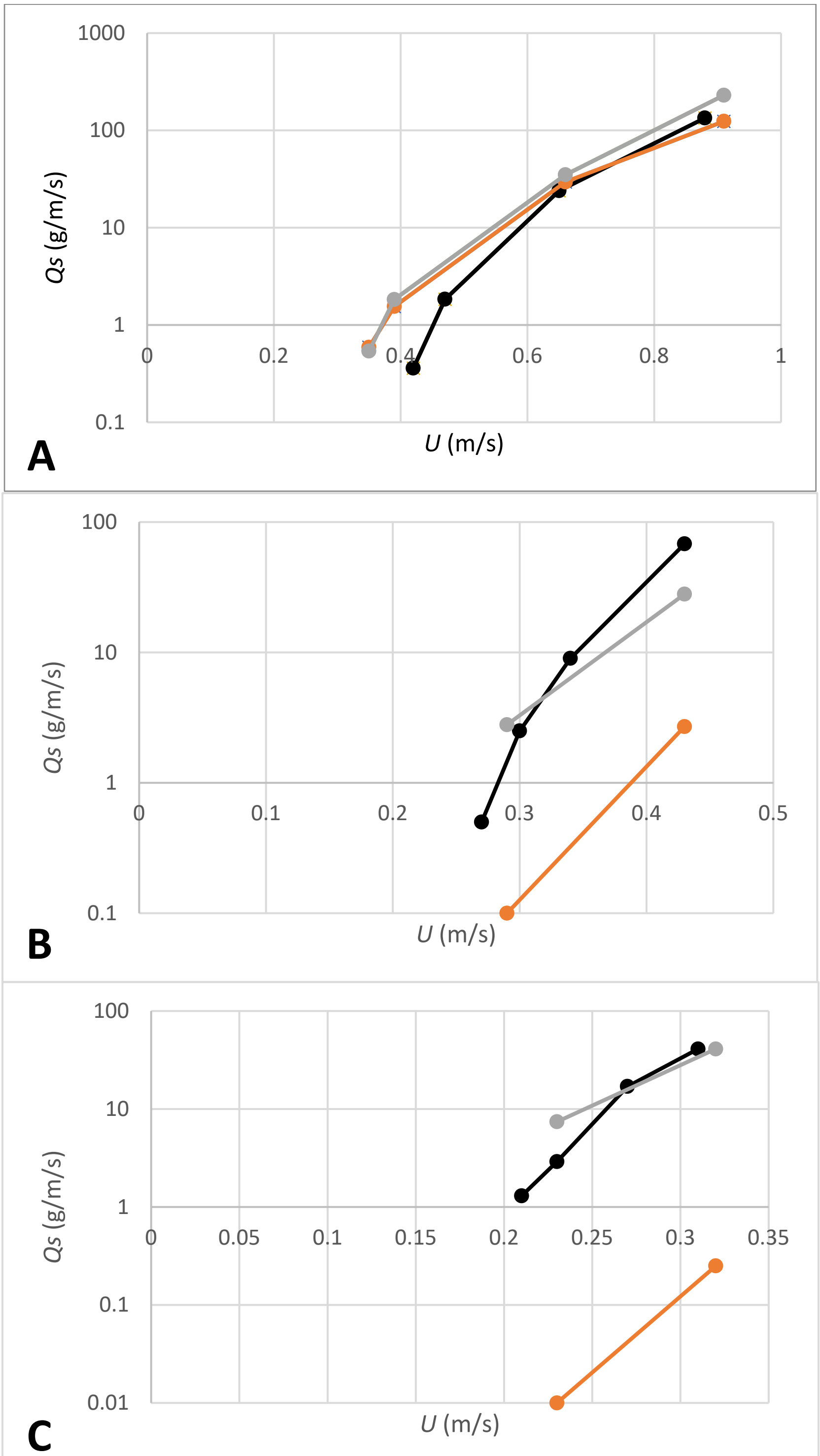

Figure 1. Bedload sediment transport rate Q_s as a function of channel velocity U for vegetation solid volume fraction $\emptyset = 0$ (panel A), $\emptyset = 0.005$ (panel B), and $\emptyset = 0.025$ (panel C). Shown in each panel are results from the Yang (2018) laboratory experiments (black), the SRH-2D simulation results (orange), and the computed sediment transport rates as proposed in Equations (10)-(15) (gray).

Discussion

The calculations demonstrate the utility of improved formulations of sediment capacity that directly account for the effect of vegetation-induced turbulence, which in turn drive mobility and transport in many vegetated flow conditions. A challenge in modeling hydraulics and sediment transport lies in the application of appropriate formulations that may vary with both the characteristics of the vegetation and the flow regime. It is expected that the formulation for computing sediment capacity proposed herein will yield improved predictions under conditions in which the production of turbulence due to flow around the vegetation stems is greater than production near the bed due to shear. Prior work suggests that for the quantity $C_D h\emptyset/(\pi d/4)$ in the range 0.01-1.0, wake production exceeds production due to shear within the cylinder array (Tanino & Nepf, 2008). However, in the case of the Yang (2018) laboratory experiments, the quantity $C_D h\emptyset/(\pi d/4)$ was in the range 1.0-5.0, which suggests that stem-generated turbulence may be important over a broader range of vegetated conditions, particularly at higher stem densities. Outside of the range of conditions for which turbulence production drives mobilization of sediment, an opposing regime is expected in which mobilization is suppressed and sediment deposition is observed (Zong & Nepf, 2010). Sediment trapping has shown to be effectively modeled by the vegetation partitioning algorithm already implemented in SRH-2D (Dombroski D. E., 2017); further study to more clearly define the modeling regimes and build appropriate logic into the model would greatly increase the applicability of the model to a range of conditions that may be observed in the natural environment and project setting. Further, the proposed modeling framework from the Yang (2018) laboratory experiments (Equations (10)-(15)) is based upon measurements of bedload transport. Additional studies should be implemented to verify the limitations of the model especially in conditions where a significant portion of the sediment may be transported in suspension.

Next Steps

The next step would be to implement the improved formulation into the SRH-2D model. Additional work should be performed to validate the use of methodology developed to model bedload transport and consider the implementation of further theory for addressing mixed-mode transport conditions. Implementing the current strategy would likely lead to improved predictions of sediment dynamics even in mixed-mode transport.

References

Baptist, M., Babovic, V., Rodriguez Uthurburu, J., Keijzer, M., Uittenbogaard, R., Mynett, A., & Verwey, A. (2007). On Inducing Equations for Vegetation Resistance. *Journal of Hydraulic Research, 45*(4), 435-450.

Brown, C. B. (1950). Sediment Transportation. *Engineering hydraulics*(12), 769-857.

Dombroski , D. E. (Draft Document in Progress). *SRH-2D Vegetation Modeling User Guide.* Denver Technical Service Center: Bureau of Reclamation.

Dombroski, D. E. (2014). *A Deterministic Spatially-Distributed Ecohydraulic Model for Improved Riverine System Management.* TSC, Denver, CO: Bureau of Reclamation.

Dombroski, D. E. (2017). *Remote Sensing of Vegetation Characteristics for Estimation of Partitioned Roughness in Hydraulic and Sediment Transport Modeling Applications.* Denver: Bureau of Reclamation Research and Development Office.

Einstein, H. A. (1950). *The bed-load function for sediment transportation in open channel flows.* US Department of Agriculture.

Gillihan, T. (2013). *Dynamic vegetation roughness in the riparian zone.* University of New Mexico.

Greimann, B., Lai, Y., & Huang, J. (2008). Two-dimensional total sediment load model equations. *Journal Hydr. Engr., 134*(8), 1142-1146.

Huang, V. H., & Greimann, B. P. (2012). *Sedimentation and River Hydraulics - One Dimension, Version 3.0.* 2012: Bureau of Reclamation Technical Service Center.

Jarvela, J. (2004). Determination of Flow Resistance Caused by Non-Submerged Woody Vegetation. *International Journal of River Basin Management, 2*(1), 61-70.

Kouwen, N., & Fathi-Moghadam, M. (2000). Friction Factors for Coniferous Trees Along rivers. *Journal of Hydraulic Engineering*, 732-740.

Kouwen, N., & Li, R.-M. (1980, June). Biomechanics of Vegetative Channel Linings. *Journal of the Hydraulics Division, Proceedings of the ASCE, 106*(HY6), 1085-1103.

Lai, Y. G. (2010). Two-Dimensional Depth-Averaged Flow Modeling with an Unstructured Hybrid Mesh. *Journal of Hydraulic Engineering, 136*(1), 12-23.

Lai, Y., & Gaeuman, D. (2013). *Bedload Adaptation Length for Modeling Bed Evolution in Gravel-Bed Rivers.* TSC, Denver, CO: Bureau of Reclamation.

Larsen, L. (2008). *Hydroecological feedback processes governing self-organization of the everglades ridge and slough landscape.* University of Colorado at Boulder, Civil Engineering.

Le Bouteiller, C., & Venditti, J. G. (2015). Sediment transport and shear stress partitioning in a vegetated flow. *Water Resources Research*, 2901-2922.

Lopez, F., & Garcia, M. (1997). Open-channel flow through simulated vegetation: Turbulence modeling and sediment transport, Wetlands Resources Program Technical Report WRP-CP-10. *US Army Corps of Engineers Waterways Experiment Station*.

Mason, D. C., Cobby, D. M., Horritt, M. S., & Bates, P. D. (2003). Floodplain friction parameterization in two-dimensional river flood models using vegetation heights derived from airborne scanning laser altimetry. *Hydrological Processes, 17*, 1711-1732.

Nepf, H. M. (1999). Drag, turbulence, and diffusion in flow through emergent vegetation. *Water Resour. Res.*, 479-489.

Nezu, I., & Onitsuka, K. (2001). Turbulent structures in partly vegetated open-channel flows with LDA and PIV measurements. *Journal of Hydraulic Research*, 629-642.

Rubey, W. W. (1933). Settling velocity of gravel, sand, and silt particles. *American Journal of Science*(148), 325-338.

Simon, A., Bennett, S., & Neary, V. (2004). Riparian Vegetation and Fluvial Geomorphology: Problems and Opportunities. In S. Bennet, & A. Simon, *Riparian Vegetation and Fluvial Geomorphology* (pp. 1-10). AGU.

Tanino, Y., & Nepf, H. M. (2008). Lateral dispersion in random cylinder arrays at high Reynolds number. *J. Fluid Mech., 600*, 339-371.

Thompson, A. M., Wilson, B. N., & Hansen, B. J. (2004). Shear stress partitioning for idealized vegetated surfaces. *Transactions of the ASAE*, 701-709.

Yang, J. Q. (2018). *Impacts of Vegetation-Generated Turbulence on Sediment Transport.* Massachusetts Institute of Technology.

Yang, J. Q., Chung, H., & Nepf, H. M. (2016). The onset of sediment transport in vegetated channels predicted by turbulent kinetic energy. *Geophysical Research Letters, 43*(21).

Zong, L., & Nepf, H. (2010). Flow and deposition in and around a finite patch of vegetation. *Geomorphology*(116), 363-372.

Appendix A – Laboratory Flume Experiments

By Qingjun Judy Yang, Ph.D., Massachusetts Institute of Technology

Experimental Setup

Laboratory experiments were conducted in a horizontal flume that recirculated water and sand separately. The flume has a 1m wide and 10m long test section. To simulate emergent vegetation, aluminum dowels with diameter $d = 6.3mm$ were fixed on perforated PVC boards in a staggered pattern and extended through the water column (Figure A 1). The number of dowels per bed area was in the range of $n = 0$ to 810 stems$/m^2$. The frontal area of the vegetation per unit volume was $a = nd = 0$ to $5.1m^{-1}$ and the solid volume fraction of the vegetation was $\phi = \pi nd^2/4 = 0$ to 0.025. Experiments with various flow rates in channels without vegetation and with vegetation of different solid volume fraction (ϕ) were carried out (Table A 1). The dowels covered the whole width ($w = 1m$) of the flume and 3 meters of the flume in the streamwise direction. The water depth h was measured in the middle of the vegetated region. The flow rate Q was measured with a flow meter with $1m^3/hr$ accuracy. The cross-sectional averaged channel velocity was calculated as $U = Q/(wh(1 - \phi))$.

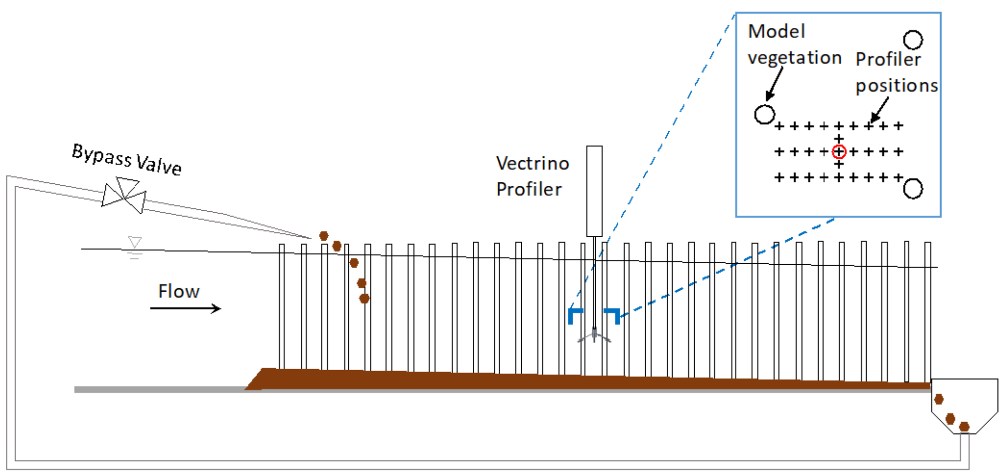

Figure A 1. The sediment-recirculating flume with model vegetation (aluminum cylinders). The near-bed flow velocity was recorded by the Vectrino profiler at 2 cm from the bed. Inset with blue edge: the top view of the region where the velocity measurements were made. 3-minute velocity measurements were recorded at multiple horizontal positions, indicated by the black pluses. The bed elevation was measured by the Vectrino profiler at the center of the diagonal between two dowels (the red circle) for 30 minutes to 2 hours to monitor the bed elevation evolution.

At the beginning of each experiment, a 4-cm thick layer of sand bed was placed on top of the PVC boards and manually flattened. The density of the sand grains was $\rho_s = 2.65g/cm^3$ and the sand diameter was in the range 0.42 to 0.60 mm with mean grain size $d_s = 0.5$ mm. Only bedload transport was observed during the experiment. Every few hours, the sand was bypassed from the sand-recirculating pipe through a three-way valve and collected in a mesh bag with 0.25mm holes. The bypassing duration ranged from 1 to 10 minutes, chosen to be long enough to ensure that the volume of the collected sand was significantly larger than the background debris in the flume. The collected sand was put into a container with water and a marked water line. The water surface in the container was maintained at the marked water line, and the dry mass of the sand was calculated from the mass difference of the container with and without the sand and the density difference between the sand and the water. The instantaneous bedload transport rate, defined as the mass of sand passing through the channel cross section per time per unit width, was calculated as the mass of the collected sand divided by the time to collect the sand and the width of the flume. We repeated the bedload measurements for at least 3 times until the cumulative moving average of all the instantaneous measurements varied by less than 10% with increasing number of measurements. The average and standard error of all the measured instantaneous bedload transport rate were used to represent the equilibrium bedload transport rate and its uncertainty, $\mathrm{Q_s} \pm \sigma_{Q_s}$ (Table A 1).

Velocity Measurements

A Nortek Vectrino profiler, an acoustic sensor that measures the velocity and the distance to the bed, was mounted on a manually-driven positioning system placed in the middle of the vegetation patch (Figure A 1). The positioning system allowed the profiler to move in the stream-wise (x), the lateral (y), and the vertical (z) directions. After the bedload transport rate reached equilibrium, the Vectrino profiler was used to measure the velocity at 0 to 4 cm relative to the bed with 1mm vertical resolution and 100Hz sampling rate for 3 minutes at multiple horizontal locations. A typical distribution of the measurement locations is indicated by the plus symbols in the inset of Fig. 1, and the number of locations is listed in the second to last column of Table A 1. Measurements at 2 cm relative to the time-mean bed elevation was used to represent the near-bed condition, because the velocity data within 2cm from the mean bed had low correlation and low signal to noise ratio (SNR) due to the interference of the bed with the acoustic signal of the profiler. For our cases, the ripple crest was up to 16mm from the mean bed, which explains why the velocity measurements closer than 2 cm from the mean bed were low quality. The velocity data was despiked, and the signal to noise ratio was larger than 30dB and the correlation was larger than 80% at 2cm from the mean bed. For each velocity record, the time-averaged velocity and turbulent kinetic energy converged to a stable value within 3 minutes. We calculated the spatial average and spatial standard deviation of multiple local measurements, which is reported in Table A 1.

Table A 1. Vegetation characteristics, sediment transport rate measurements, and flow characteristics measured in this study.

Case Number	Vegetation Frontal Area per Unit Canopy Volume	Vegetation Solid Volume Fraction	Flow Rate	Water Depth	Bedload Transport Rate	Spatial-ave TKE (# of profiles)	Reynolds stress
	a (m^{-1})	ϕ	U (m/s)	h (m)	$Q_s \pm \sigma_{Q_s}$ $(g/s/m)$	$k_t \pm \sigma_{k_t}$ (cm^2/s^2)	$(\tau_{RS} \pm \sigma_{RS})/\rho$ (cm^2/s^2)
Bare Channel							
1.1	0	0	0.42	0.12	0.36 ± 0.05	28 ± 1 (8)	3.9 ± 0.2
1.2	0	0	0.47	0.12	1.84 ± 0.08	46 ± 1 (34)	6.0 ± 0.2
1.3	0	0	0.65	0.12	24 ± 1	111 ± 11 (8)	14.7 ± 1.3
1.4	0	0	0.88	0.12	134 ± 8	205 ± 10 (8)	12.8 ± 1.6
Channels with Emergent Vegetation							
2.1	1.1	0.005	0.27	0.12	0.5 ± 0.1	19 ± 3 (24)	0.5 ± 0.2
2.2	1.1	0.005	0.30	0.12	2.5 ± 0.3	20 ± 2 (24)	0.2 ± 0.2
2.3	1.1	0.005	0.34	0.12	9 ± 1	32 ± 5 (24)	1.9 ± 0.5
2.4	1.1	0.005	0.43	0.12	68 ± 17	65 ± 8 (24)	6.2 ± 0.7
3.1	2.5	0.012	0.21	0.12	0.15 ± 0.02	17 ± 2 (27)	0.5 ± 0.1
3.2	2.5	0.012	0.24	0.12	2.6 ± 0.5	22 ± 2 (27)	0.1 ± 0.1
3.3	2.5	0.012	0.28	0.12	9.4 ± 0.6	45 ± 5 (27)	2.0 ± 0.6
4.1	5.1	0.025	0.21	0.10	1.3 ± 0.1	20 ± 2 (23)	0.5 ± 0.1
4.2	5.1	0.025	0.23	0.10	2.9 ± 0.3	42 ± 4 (23)	0.1 ± 0.1
4.3	5.1	0.025	0.27	0.10	17 ± 1	46 ± 4 (23)	1.0 ± 0.2
4.4	5.1	0.025	0.31	0.10	41 ± 2	51 ± 5 (23)	1.6 ± 0.3

Appendix B – SRH Hydraulic and Mobile Bed Model

An SRH-2D hydraulic and mobile bed sediment model was built to simulate the experiments conducted in the laboratory flume (Appendix 1). The model is based on a 1 m wide by 10 m long rectangular grid comprised of 2000 quadrilateral cells (Figure B 1). The elevation of every cell in the mesh was set to zero base elevation, although the mobile bed was initiated with a 4 cm thick layer of sand and 0.5 cm active layer. A single gradation was specified having a minimum, maximum, and median grain diameter of 0.42, 0.6, and 0.5 mm, respectively.

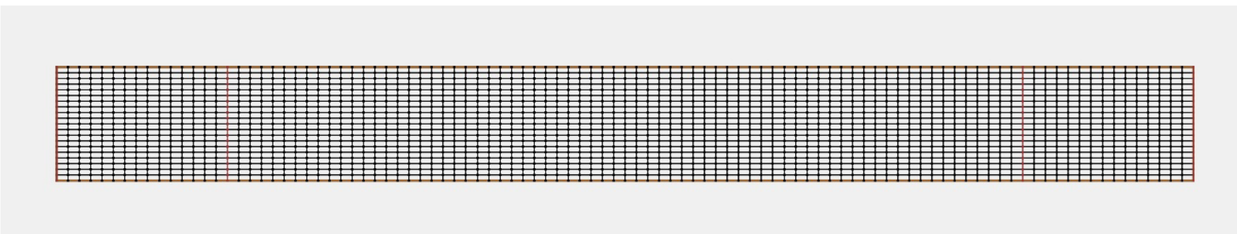

Figure B 1. Plan view of computational mesh used in the SRH-2D model. The mesh is 1 m wide by 10 m long and composed of 2000 elements.

The input sediment rate was determined by transport capacity. The inlet discharge, exit water surface elevation, roughness, and sediment transport capacity formula were systematically varied through the model calibration and validation process.

The model was calibrated to the bare bed (non-vegetated) flume experiments. For the non-vegetated simulations, a constant roughness was specified over the model domain. The model was considered calibrated when the mean velocity, depth of flow, and sediment transport rate approximately matched that reported in the results of the flume experiments (Table A 1).

Observations of the flume experiments noted that sediment was transported only as bedload. The total load transport equations (8) and (9) can be constrained to a bedload-only mode (f_k=0) by specifying “ST_MODE=BED” in the *casename*_SIF.dat model input file. To more closely model the experimental observations, the bedload mode was tested in the SRH-2D simulations. Through varying capacity formulas and discharge, the model unexpectedly predicted greater total transport when the equations were constrained to the bedload-only mode. Without exploring the result further, calibration and validation simulations were conducted using the total load mode.

The results of calibrating the SRH-2D mobile bed sediment and hydraulic model to the bare bed, non-vegetated flume experiments are shown in Table B 1. The Case Number listed in the left-most column corresponds to the Case Number of the experiment results presented in Table A 1. The Parker (1990) transport capacity formula demonstrated proficiency, although the Wilcock & Crowe (2003) formula was most adept in reproducing the experimental transport rates for an unvarying roughness across flow rates.

The effect of vegetation on the hydraulics and sediment transport was modeled using several approaches. The Wilcock & Crowe (2003) formulation was selected for calculating transport capacity based on the calibration results. Table B 2 presents the configuration employed for attempting to model vegetation using a blocked obstruction methodology in SRH-2D. The blocked obstruction is a drag-force based technique for modeling the hydraulic effect of flow around solid objects. The results were inconclusive because of the coarseness of the mesh relative to the size of the vegetation elements (defined as obstructions) leading to its inability to appropriately resolve the obstructions. It is logically presumed that realistic simulation of a collection of blocked obstructions would require that the individual elements be at least approximately resolved by the computational mesh, which is not tractable for the case of vegetated flow conditions. Table B 3 presents results from the hydraulic and mobile bed model using the partitioned roughness methodology for inclusion of vegetation affects (Dombroski D. E., 2017). Formulas for computing the component of roughness (Dombroski D. E., Draft Document in Progress) associated with the vegetation included Baptist (2007), Kouwen (2000), and static. Presented in the table are both the grain roughness n_o component and the total roughness n_t (from which the vegetation roughness n_v can be calculated). The Jarvela (2004) formula for calculating roughness was not used because the approach is intended for leafy vegetation and includes the leaf area index (LAI) parameter, which makes little physical sense in modeling simplified stems represented as dowels. The Kouwen (2000) approach lacks a direct stem density parameter and therefore proved too simplistic for practical application in modeling the flume experiments for varying vegetation solid volume fraction ϕ. The static partitioned roughness approach does not calculate a dynamic roughness but instead depends on the user to specify a constant vegetation roughness n_v. In comparison with the laboratory experiments, the results demonstrate that the model vastly underpredicts the sediment transport rate, regardless of the chosen formula for estimating vegetative roughness. In the model, the total roughness is used to calculate the hydraulic variables while only the grain roughness component is used to compute sediment transport capacity (Dombroski D. E., 2017). The approach approximates the effect of sediment trapping, which effectively reduces the fluid capacity to move sediment, without consideration of potential for capacity enhancement due to vegetation-generated turbulence.

Table B 1. Calibration results of mobile bed model simulations for bare bed (non-vegetated) conditions.

Case Number	Vegetation Frontal Area per Unit Canopy Volume	Vegetation Solid Volume Fraction	Flow Rate	Water Depth	Bedload Transport Rate	Roughness	Notes
	a (m^{-1})	ϕ	U (m/s)	h (m)	$Q_s \pm \sigma_{Q_s}$ $(g/s/m)$	*n*	
Capacity Formula: Parker (1990)							
1.1		0	0.42	0.12	1.8	0.015	
1.4		0	0.85	0.13	130	0.015	
Capacity Formula: Wu et al. (2000)							
1.4		0	0.8	0.3	90	0.019	unstable
Capacity Formula: Engelund & Hanson (1972)							
1.4		0	0.87	0.28	122	0.019	Slightly unstable
Capacity Formula: Wilcock & Crowe (2003)							
1.1		0	0.35	0.13	0.59	0.016	
1.2		0	0.39	0.13	1.55	0.016	
1.3		0	0.66	0.14	29.5	0.016	
1.4		0	0.91	0.14	124	0.016	
Capacity Formula: Yang (1979)							
1.4		0	0.71-0.88	0.28	970	0.019	Dune formation, unstable

Table B 2. Configuration employed for attempting to model vegetation using a blocked obstruction methodology in SRH-2D.

Case Number	Vegetation Frontal Area per Unit Canopy Volume	Vegetation Solid Volume Fraction	Flow Rate	Water Depth	Bedload Transport Rate	Roughness	Notes
	a (m^{-1})	ϕ	U (m/s)	h (m)	$Q_s \pm \sigma_{Q_s}$ $(g/s/m)$	*n*	
Method: Blocked Obstructions							
2.4		0.005				0.016	475 obstructions

Table B 3. Simulation results of mobile bed simulations for vegetated conditions.

Case Number	Vegetation Frontal Area per Unit Canopy Volume	Vegetation Solid Volume Fraction	Flow Rate	Water Depth	Bedload Transport Rate	Roughness	Notes
	a (m^{-1})	ϕ	U (m/s)	h (m)	$Q_s \pm \sigma_{Q_s}$ $(g/s/m)$	n_o, n_t	
Roughness Formula: Baptist (2007)							
2.1		0.005	0.29	0.12	0.1	0.016, 0.07	
2.4		0.005	0.43	0.15	2.7	0.016, 0.08	
4.1		0.025	0.23	0.09	0.01	0.016, 0.11	
4.4		0.025	0.32	0.14	0.25	0.016, 0.15	
Roughness Formula: Kouwen (2000)							
2.1		0.005	0.28	0.12	0.1	0.016, 0.059	No way to adjust density
2.4		0.005	0.45	0.13	3.7	0.016, 0.058	No way to adjust density
Roughness Formula: Static Partitioned Roughness							
2.1		0.005	0.29	0.12	0.1	0.016, 0.051	
2.4		0.005	0.44	0.13	3.7	0.016, 0.05	